

# The Dynamic Nonlinear Behavior of Fly Photoreceptors Evoked by a Wide Range of Light Intensities

A. S. French,\* M. J. Korenberg,‡ M. Järvillehto,§ E. Kouvalainen,¶ M. Juusola,¶ and M. Weckström¶

\*Department of Physiology, University of Alberta, Edmonton, Alberta, Canada; ‡Department of Electrical Engineering, Queen's University, Kingston, Ontario, Canada; §Department of Zoology, University of Oulu, Oulu, Finland; and ¶Department of Physiology, University of Oulu, Oulu, Finland

**ABSTRACT** Fly photoreceptor cells were stimulated with steps of light over a wide intensity range. First- and second-order Volterra kernels were then computed from sequences of combined step responses. Diagonal values of the second-order Volterra kernels were much greater than the off-diagonal values, and the diagonal values were roughly proportional to the corresponding first-order kernels, suggesting that the response could be approximated by a static nonlinearity followed by a dynamic linear component (Hammerstein model). The amplitudes of the second-order kernels were much smaller in light-adapted than in dark-adapted photoreceptors. Hammerstein models constructed from the step input/output measurements gave reasonable approximations to the actual photoreceptor responses, with light-adapted responses being relatively better fitted. However, Hammerstein models could not account for several features of the photoreceptor behavior, including the dependence of the step response shape on step amplitude. A model containing an additional static nonlinearity after the dynamic linear component gave significantly better fits to the data. These results indicate that blowfly photoreceptors have a strong early gain control nonlinearity acting before the processes that create the characteristic time course of the response, in addition to the nonlinearities caused by membrane conductances.

## INTRODUCTION

The gain of phototransduction in vertebrates and invertebrates can vary over a range of about  $10^9$  in order to cope with a similar range of ambient light intensities. This gain control, or adaptation, consists of several processes with time courses varying from milliseconds to days (Järvillehto, 1979; Autrum, 1981; Fein and Szuts, 1982; Classen-Linke and Stieve, 1986; Laughlin, 1989). In insects, such gain control can occur with stimuli of only a few photons (Dubs, 1981; French and Kuster, 1985; Grzywacz and Hillman, 1985). Recently, one of these processes has been identified as voltage-activated ion channels that reduce the change in membrane potential by shunting the light-gated current (Laughlin and Weckström, 1989; Weckström et al., 1991; Hardie et al., 1991; Pece and French, 1992).

Adaptive gain control represents a strongly nonlinear behavior, but there is also a significant time dependence because the response to brief flashes (or even to a single photon) is a voltage change that grows and decays over a period of hundreds of milliseconds. Therefore, photoreceptors behave as dynamic nonlinear systems and require appropriate techniques for their analysis. Surprisingly, previous investigations have yielded only a small second-order nonlinear contribution to the response (Eckert and Bishop, 1975; Gemperlein and McCann, 1975; Marmarelis and McCann, 1977; Pece et al., 1990) or pointed to an almost totally linear system (French and Järvillehto, 1978; French, 1980; Weckström et al., 1988). The method used in these studies, and a

popular general method for analyzing dynamic nonlinear systems, is to use a random or pseudo-random stimulus and measure the Wiener kernels (Marmarelis and Marmarelis, 1978; Sakai, 1992). With this method it is necessary to add the random stimulus to a continuous background light intensity, which seems to effectively linearize the photoreceptor behavior (Juusola, 1993).

An alternative approach, which we used here, is to estimate the Volterra kernels of the system using non-Gaussian stimuli that are well suited to the nonlinearities being investigated. Several methods have been developed recently for such analysis (Korenberg, 1982, 1988). Using this approach, a wide range of possible input signal waveforms can be used, but they must be sufficiently rich in amplitude and time course to explore the behavior of the system in the regions of interest. Here, we presented steps of light to dark-adapted photoreceptors and step increments or decrements of light intensity to light-adapted photoreceptors, with a wide range of step amplitudes. The individual responses were then combined to form sets of input/output data that were used to obtain Volterra kernels. With this procedure we were able to characterize the dynamic nonlinear behavior but inevitably had to ignore processes that were significantly slower than the durations of the stimuli. The Volterra kernels were used to produce nonlinear models that could account for the complete set of step responses, and these suggest a sequence of several distinct processes within fly photoreceptors that are qualitatively different under dark- and light-adapted conditions.

Received for publication 6 January 1993 and in final form 21 April 1993.

Address reprint requests to Dr. A. S. French, Department of Physiology, University of Alberta, Edmonton, Alberta T6G 2H7, Canada.

© 1993 by the Biophysical Society

0006-3495/93/08/832/08 \$2.00

## MATERIALS AND METHODS

Flies (*Calliphora vicina*) were obtained from a laboratory culture. Adults and larvae were fed on liver, yeast, and sucrose, and the stock was refreshed

regularly with wild flies. Each fly was attached with beeswax onto a platform with a rotating Cardan arm, and a silver chloride reference electrode was mounted in the head. Ventilation was maintained by leaving the abdomen intact with spiracles functioning normally. Dark-adapted flies were kept in complete darkness for at least 30 min before beginning a recording.

Glass microelectrodes were filled with 3 M potassium acetate and 5 mM potassium chloride and had resistances of  $\sim 150$  M $\Omega$ . Electrodes were mounted on a piezoelectric microtranslator (Burleigh PZ-550 inchworm controller) and entered the compound eye through a small lateral hole that was sealed with high-vacuum grease. Membrane potentials were recorded with an intracellular amplifier (SEC-1L; NPI Electronic, Tamm, Württemberg Germany) operating in the balanced bridge mode. Recordings were made from R1-6 photoreceptor somata, identified by criteria published previously (Järvilehto and Zettler, 1970; Hardie, 1979). Experiments were performed at room temperature ( $\sim 20^\circ\text{C}$ ).

Light stimuli were provided by a green light emitting diode (Stanley HBG5666X, with peak emission at 555 nm) driven by a linearized voltage-to-current convertor. The light stimulus was calibrated by counting the voltage responses (single bumps) caused by the absorption of single photons. For this purpose, the intensity was attenuated with neutral density filters (Kodak Wratten, Rochester, NY). The stimulation protocols were produced by a computer program in the ASYST programming language (Keithley, Taunton, MA).

Nonlinear system identification was performed by measuring the Volterra kernels via the parallel cascade method (Korenberg, 1982). A detailed description of the parallel cascade technique and its use to obtain Volterra kernels has been provided by Korenberg (1991). The digitized signals were assumed to come from an unknown system with discrete input,  $x_n$ , and output,  $y_n$ , where  $t$  is time, that could be approximated by a set of parallel nonlinear cascades. The first component in each cascade path was a dynamic linear system with impulse response  $g_{n,u}$ , and the second component was a polynomial function with coefficients  $c_{n,i}$ , where  $n$  is the cascade number,  $u$  is discrete time, and  $i$  is the polynomial order. The parallel cascade method also allows further alternating dynamic linear and static nonlinear systems to be optionally inserted in each path, but these were omitted here. After each new cascade was added, the mean square error of the residual signal,  $y_{n,r}$ , was calculated from

$$e_{n+1} = \frac{\bar{y}_{n,r}^2}{\bar{y}_r^2} \quad (1)$$

where the bars indicate mean values, taken over  $t$ .

The output of the unknown system,  $y_n$ , was considered as a Volterra series:

$$y_t = K_0 + \sum_u K_{1,u} x_{t-u} + \sum_u \sum_v K_{2,u,v} x_{t-u} x_{t-v} + \dots \quad (2)$$

and the Volterra kernels,  $K_0$ ,  $K_1$ , etc. were calculated from the parallel cascade components (Korenberg, 1982, 1991). In performing the parallel cascade measurements and constructing the Volterra kernels, the polynomial functions were restricted to second order to prevent over-fitting the experimental data, which normally contained about 1500 independent data points.

## RESULTS

### Dark-adapted step responses

Fig. 1 shows the membrane potential changes in a dark-adapted fly photoreceptor produced by a series of seven different amplitude steps in light intensity, ranging from  $7.5 \times 10^{-7}$  to  $2.4 \times 10^{-6}$  effective photons/s (ep/s). Each step was of 200 ms duration. The membrane potential response was stored at 5-ms intervals during the step and for the following 700 ms. In order to reduce the photon noise in the response and avoid light adaptation, responses were averaged to 10 identical steps at each amplitude, with a period of 20 s between each step presentation. The averaged responses to the different stimulation steps were then combined with the ap-

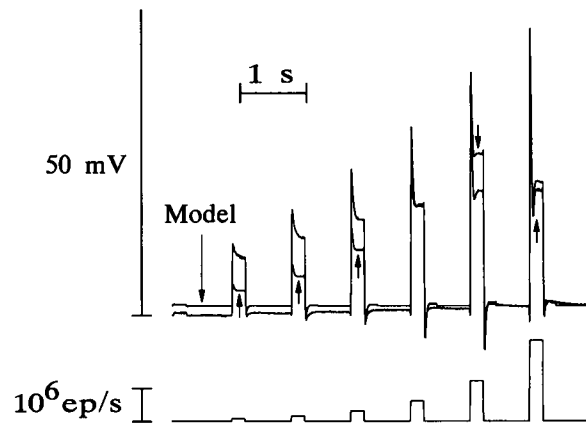


FIGURE 1 The responses of a dark-adapted fly photoreceptor to 7 steps of light with increasing amplitude. The light stimuli are shown below in effective photons/s (ep/s). An effective photon is one that is absorbed and transduced by the photoreceptor. Each step response was obtained by averaging the responses to 10 identical step stimuli. The step responses were collected separately and then combined numerically to form this ascending series. The actual interstimulus interval between the light stimuli was always 20 s. Superimposed on the experimental responses is the predicted output of the parallel cascade model to the same series of steps. Arrows indicate the model prediction.

propriate stimuli to form the data of Fig. 1. These responses are comparable to previous descriptions of the step responses of dark-adapted fly photoreceptors (French, 1979; Järvilehto, 1979; Autrum, 1981; Laughlin, 1981; Hardie, 1985).

The need to gather many step responses made it impossible to obtain truly dark-adapted responses within the experimental time available. However, the term “dark adapted” will be used here to describe photoreceptors that were initially dark adapted and then held in the dark for a period of 20 s between light stimuli.

The responses of the dark-adapted photoreceptor shown in Fig. 1 were fitted by the parallel cascade model using a memory length of 200 ms (40 points with a 5-ms separation) for the dynamic linear components. Each cascade had a second-order polynomial nonlinear component. The output of the parallel cascade model is shown as an additional trace in Fig. 1, with arrows marking the model prediction where necessary. The final mean square error from Eq. 1 was 11.82%. One source of error was the mean level of the prediction for small step inputs. The reason for this is the presence of slower time course processes that are evident at the ends of the larger steps. These prolonged after-depolarizations have been reported before (French, 1979; Hardie, 1985) and could not be fitted by the model because of its limited memory. Therefore, they produced an apparent elevation in the mean level of the output with zero input.

Apart from the mean prediction level, it is clear that a second-order Volterra series was inadequate to describe the step responses of Fig. 1, suggesting that the system has higher-order nonlinearities. However, the use of higher-order nonlinearities in the cascades could not be justified by the restricted data set available in this case.

The parallel cascades were used to obtain the first- and second-order Volterra kernels. Figs. 2 and 3 show the kernels

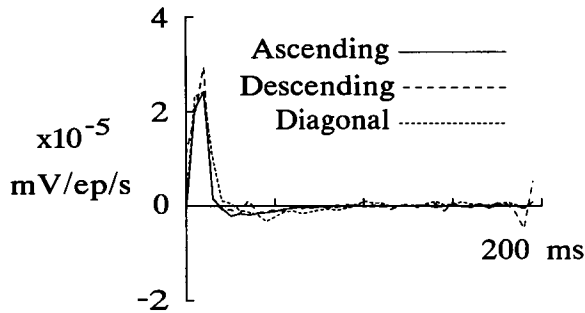


FIGURE 2 The first-order Volterra kernel of the dark-adapted photoreceptor obtained from the parallel cascade model for the ascending steps of Fig. 1 (solid line) and for the same steps arranged in descending order (long dashes). The diagonal of the second-order kernel is also shown (short dashes) after normalization to the same peak amplitude as the first-order kernels.

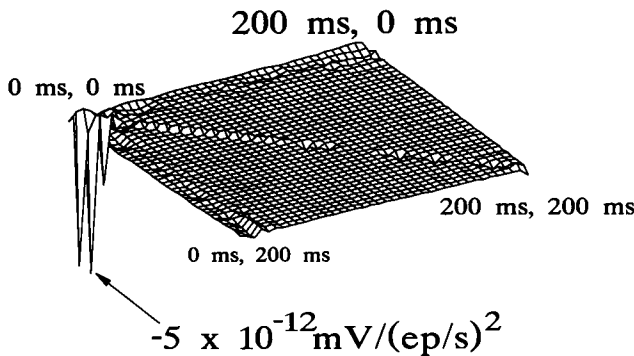


FIGURE 3 The second-order Volterra kernel of the dark-adapted photoreceptor obtained from an ascending series of light steps. The figure shows the lower surface of a three-dimensional perspective plot. Most of the data lie in a plane that is close to zero. The amplitude of the largest absolute value is indicated. These data were not smoothed or interpolated.

obtained from the same model as used in Fig. 1. The first-order kernel had a form similar to those measured previously by flash and white noise stimuli (Eckert and Bishop, 1975; Gemperlein and McCann, 1975; Marmarelis and McCann, 1977; Weckström et al., 1988). The effectiveness of the parallel cascade model, and the kernels obtained, were independent of the order in which the step responses were combined. The solid line in Fig. 2 shows the first-order kernel obtained by arranging the steps in ascending amplitude order (Fig. 1). The line of long dashes shows the kernel obtained by arranging the steps in decreasing amplitude order. Here, the parallel cascade model gave a similarly good fit with 8.24% mean square error, and the first-order kernel was almost identical to that obtained from the ascending data.

The second-order kernel also had a reliable form. It was largely restricted to the diagonal,  $u = v$ , and along the diagonal its form was approximately a negative copy of the first-order kernel. Fig. 3 shows the lower surface of a projected image of the second-order kernel obtained from the ascending steps. The diagonal of this kernel is also plotted (short dashes) with the first-order kernels in Fig. 2, after inverting its sign and normalizing to the same amplitude as

the first-order kernel. The diagonal was similar but not identical to the first-order kernels.

The Hammerstein cascade model (Fig. 4) is a dynamic nonlinear system consisting of a static nonlinearity followed by a linear filter (Korenberg 1973; Hunter and Korenberg, 1986). A Hammerstein system has a second-order kernel that is zero-valued except along the diagonal,  $u = v$ , where it has the same form as the first-order kernel. These are necessary but not sufficient conditions for the system to be Hammerstein (Korenberg, 1973; Hunter and Korenberg, 1986). Since these conditions were approximately satisfied in this case, we attempted to fit the data by a Hammerstein model. The linear filter,  $g_j$ , was obtained from the first-order kernel (Hunter and Korenberg, 1986), and the static nonlinearity was modeled as a polynomial series using a Gram-Schmidt procedure (Korenberg et al., 1988). Here, and in the NLN model described below, we used sixth-order polynomials as a compromise between accuracy, stability, and computation time.

Fig. 5 shows the prediction of the resulting Hammerstein model for the data of Fig. 1. The Hammerstein model gave a better overall approximation to the response (mean square error = 3.23%). However, its failure to predict the change in shape of the response at different amplitudes is a direct consequence of its structure, because all of the time-dependent behavior is linear at the end of the cascade. It also produced exaggerated negative overshoots at the end of each step.

Although the Hammerstein model gave a better fit to the data than a second-order Volterra system, there is significant evidence available for nonlinearities at the end of the phototransduction process. These include self-shunting of the light-induced conductance and voltage-activated conductances (Laughlin, 1981; Laughlin and Weckström, 1989; Weckström et al., 1991; Pece and French, 1992; Tsukahara, 1980). We therefore added a second static nonlinear component to the Hammerstein model to produce the nonlinear/linear/nonlinear sandwich model (NLN model) shown in Fig. 4. The model was fitted to the data using the Levenberg-Marquardt general nonlinear technique (Press et al., 1990). The NLN model of Fig. 4 was used as the nonlinear function,

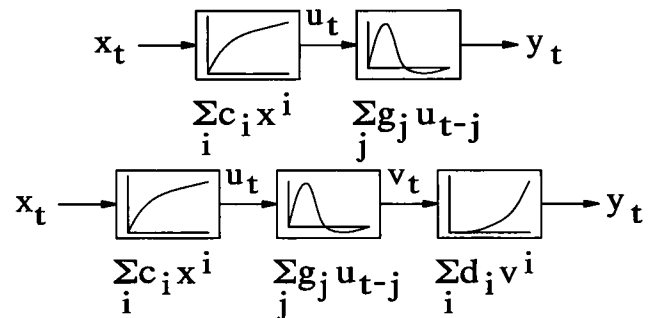


FIGURE 4 Block diagrams of the Hammerstein (top) and NLN (bottom) nonlinear dynamic models. The Hammerstein model consists of a cascade of a static nonlinear component, represented here by a polynomial with coefficients  $c_i$ , followed by a linear dynamic system with impulse response  $g_j$ . For the NLN model an additional nonlinear static component, with polynomial coefficients  $d_i$ , was added.

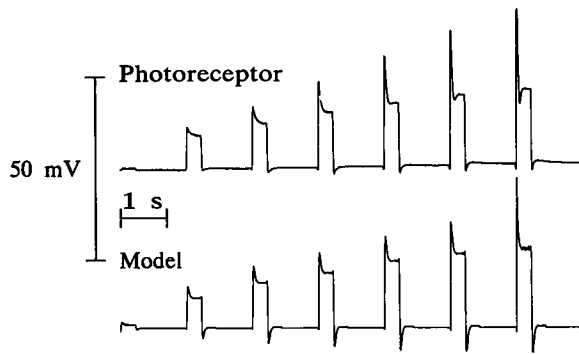


FIGURE 5 The predicted output of the Hammerstein model of Fig. 4 for the dark-adapted responses of Fig. 1. The Hammerstein model fits the plateau regions quite well but cannot reproduce the change in time course of the step responses and has excessive negative overshoots after the steps. The traces have been separated vertically because of their close similarity.

and the parameters to be fitted consisted of the coefficients of the polynomials ( $c_i$  and  $d_i$ ) and the 40 values of the linear component ( $g_j$ ). Initial estimates of the parameters were obtained from the Hammerstein model for  $c_i$  and  $g_j$ . Parameter  $d_1$  was initially set to unity, and all other values of  $d_i$  were initially set to zero.

The algorithm converged successfully to give the prediction shown in Fig. 6. The mean square error was now reduced to 1.55%. Note that the NLN model was able to predict part of the change in time course of the different amplitude steps, and it reduced the negative overshoots.

**Light-adapted step responses**

The responses of a light-adapted photoreceptor to 10 different steps of both positive and negative amplitudes are shown in Fig. 7, together with the predicted response from a parallel cascade model. Here, cascades were used with second-order polynomial functions, and the final mean square error was 1.16%. The background light intensity during the recordings was  $10^6$  ep/s, which produced a depolarization of approximately 20 mV. This can be compared to the dark-adapted response of Fig. 1, where a flash of  $1.2 \times 10^6$  ep/s produced

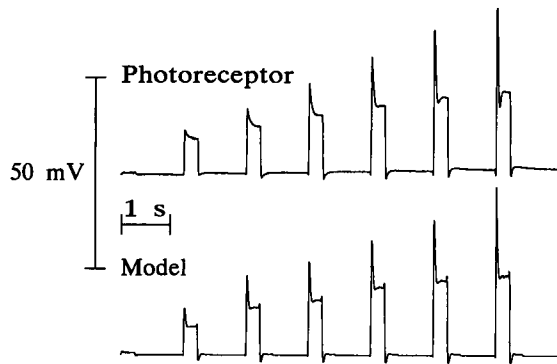


FIGURE 6 The predicted output of the NLN model of Fig. 4 for the dark-adapted responses of Fig. 1. Note the improved prediction over the Hammerstein model.

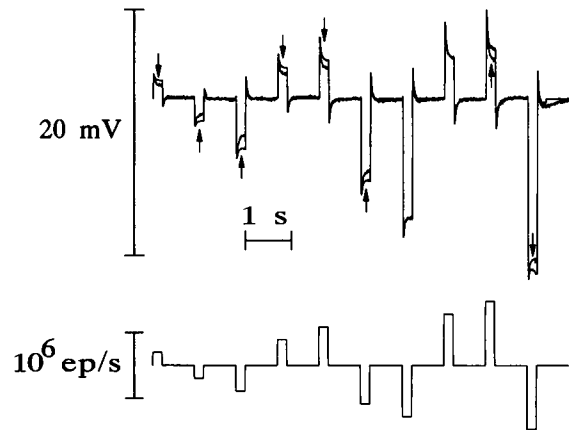


FIGURE 7 The responses of a light-adapted fly photoreceptor to 10 steps of light with both positive and negative amplitudes. The light stimuli are shown below. They were added to a constant background intensity of  $10^6$  ep/s, which produced a mean depolarization of 20 mV. Each trace was obtained by averaging the responses to 10 identical step stimuli. Superimposed on the experimental data is the predicted output of the parallel cascade model (arrows) to the same series of steps.

a plateau response of 19.4 mV. The absolute amplitudes of the steps ranged from  $0.2$  to  $1.0 \times 10^{-6}$  ep/s. The model prediction in this case was closer than for the dark-adapted experiment, but there were still substantial errors.

First- and second-order Volterra kernels were calculated from the parallel cascade model. The second-order kernel was again limited mainly to the diagonal,  $u = v$ , although it was  $\sim 50$  times smaller than the corresponding kernel from the dark-adapted photoreceptor and more variable. This was expected because light-adapted photoreceptors behave relatively linearly (Juusola, 1993). Hammerstein and NLN models were fitted to the light-adapted data using procedures identical to those followed for the dark-adapted responses. The resulting NLN model prediction, with a final mean square error of 0.67%, is shown in Fig. 8.

**NLN model components**

Fig. 9 shows the linear components ( $g_j$ ) obtained from the NLN models of both the dark- and light-adapted step re-

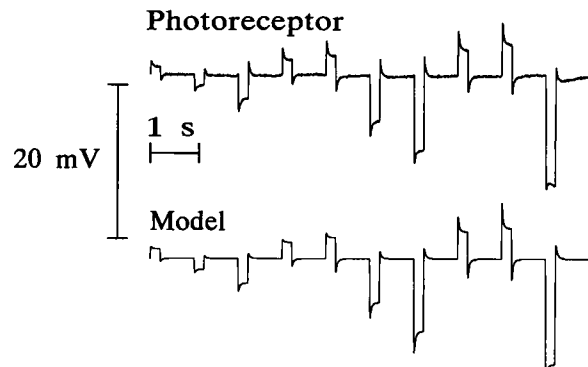


FIGURE 8 The predicted output of the NLN model of Fig. 4 for the light-adapted photoreceptor responses of Fig. 7. The traces have been separated vertically because of their close similarity.

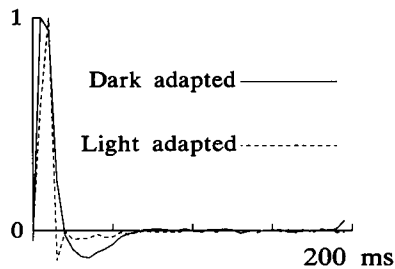


FIGURE 9 The linear components,  $g_j$ , of the NLN models for the dark-adapted and light-adapted responses (Figs. 6 and 8). Both responses have been normalized to a maximum amplitude of 1 (see text).

sponses. These components have forms similar to those of the well-known flash responses of fly photoreceptors. Dark-adapted and light-adapted components have been normalized to the same amplitude. In a sandwich model of this form, it is impossible to estimate the actual amplitudes of the separate components because linear scaling elements could be present at any arbitrary stage of the model without affecting its overall behavior. At this temporal resolution, there was not a large difference in the time to peak of the two responses; in fact the light-adapted response was slightly slower. However, the dark-adapted response had a longer total duration, not settling to zero until  $\sim 75$  ms, in comparison with  $< 50$  ms for the light-adapted response.

The first nonlinear components ( $c_i$ ) of the NLN models for dark- and light-adapted cells are plotted together in Fig. 10. Here, the polynomials were calculated for the same input ranges, in effective photons/s, as were used in the actual experiments, so that their alignment along the abscissa is correct. However, their outputs have been linearly scaled to a maximum of unity. The dark-adapted component was strongly nonlinear, rising rapidly for small flashes and then saturating to large flashes. Fig. 10 probably underestimates the sharpness of this nonlinearity because it was limited to a sixth-order polynomial. In contrast, the light-adapted component was much more linear, as expected. For both components, the value at the highest intensity stimulus deviated from the main trajectory. This might reflect inadequacies of the model structure or the polynomial order in dealing with the highest input values.

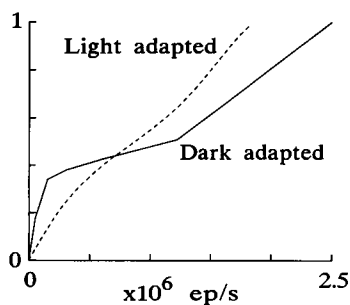


FIGURE 10 The first (input) static nonlinearity obtained from the components,  $c_i$ , of the NLN models for the dark- and light-adapted responses. Both functions were evaluated over the actual input light intensity ranges, but their outputs have been linearly normalized to a maximum value of unity.

For the second polynomial component, the dark-adapted cell was also strongly nonlinear (Fig. 11). However, the nonlinearity was in a direction opposite to that of the compression of Fig. 10. For the two curves of Fig. 11, the ordinates were aligned to correspond to the actual outputs of the model, but the positions of the curves along the abscissa are arbitrary. Since the mean stimulus to the light-adapted cell and a flash of the same intensity to the dark-adapted cell produced similar plateau depolarizations of about 20 mV, the two curves were aligned to intersect at 20 mV.

The dark-adapted nonlinearity was well approximated by a second-order polynomial. The curve in Fig. 11 is from a third-order polynomial fit, but the third-order term was small, changing the highest value by only 8%. Addition of a fourth-order term did not significantly improve the fit. In contrast, the light-adapted nonlinearity was more complex, increasing faster than linearly for low intensities and then compressing the responses to the strongest stimuli. The curve shown is from a fourth-order polynomial fit.

## DISCUSSION

### The modeling rationale

A complete model of a dynamic nonlinear system would be able to predict the system's output to any input signal. In the case of fly phototransduction dynamics, reaching this goal has been prevented so far by several fundamental problems. The photoreceptors operate over a wide range of light intensities and change their gain and time-dependent properties accordingly. In previous modeling studies this difficulty has been overcome by limiting the range of stimuli. The white noise approach (Marmarelis and Marmarelis, 1978), although the method of choice in many cases, effectively excludes dark-adapted responses. Light adaptation seems to linearize the fly phototransduction system (Juusola, 1993), while kernels calculated from paired flashes (e.g., Pece et al., 1990) are generally not least-squares estimates. Here, we estimated Volterra kernels with the parallel cascade method (Korenberg, 1982, 1991), using step changes in light intensity, under both dark- and light-adapted conditions.

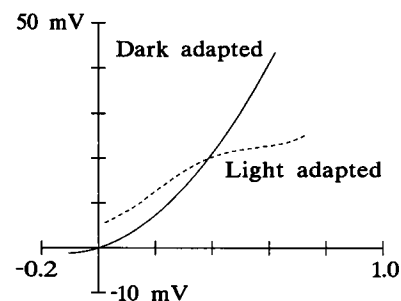


FIGURE 11 The second (output) static nonlinearity obtained from the components,  $d_i$ , of the NLN models for the dark-adapted and light-adapted responses. Both functions have been linearly normalized to correspond to the actual output voltages. However, their relative positions along the abscissa are arbitrary.

The responses of insect photoreceptors to steps of light have a characteristic form that is well documented (Järvilehto, 1979; Autrum, 1981; Laughlin, 1981; Hardie, 1985), although the underlying dynamics are still poorly understood. The earliest ideas were focused on linear models in both vertebrates (Baylor et al., 1974) and invertebrates (Fuortes and Hodgkin, 1964; Pinter, 1966; Zettler, 1969), but later models have included either nonlinear transformations, as in the log-normal model of Payne and Howard (1980), or nonlinear feedback (French, 1980). We used the parallel cascade method to estimate the Volterra kernels, which allowed a relatively large number of lagged values to be obtained with a limited computer memory. The method also allowed continuous monitoring of the residual mean square error of the model and the kernel values, as additional cascades were added during analysis. This approach enabled us to analyze phototransduction in both dark- and light-adapted photoreceptors. Light-adapted photoreceptors reflect the normal physiological condition quite closely, because blowflies are mainly active during full daylight conditions, where naturally occurring light contrasts are restricted to a range of about  $-1$  to  $+1$  (Laughlin, 1981, 1989). On the other hand, step responses in dark-adapted photoreceptors are bound to be dominated by the nonlinear components that convert the phototransduction machinery from the dark-adapted to the light-adapted state.

The NLN model gave a reasonable approximation to the system behavior over a wide range of stimulus intensities, although the fit was much better when the photoreceptors were light-adapted. The model suggests that fly photoreceptors perform nonlinear operations both early and late in the phototransduction process. Strong nonlinear compression, as seen here, is a useful operation in a system requiring high gain and wide operating range. It is particularly desirable at the input, where it can compress the range of signals entering the dynamic amplifier and allow it optimum gain.

### The light-adapted photoreceptor

As noted in several previous investigations (French, 1980; Weckström et al., 1988; Järvilehto et al., 1989; Juusola, 1993), the light-adapted fly photoreceptor had less significant nonlinearities than the dark-adapted one, as seen in the small amplitude of the second-order kernel. Correspondingly, the input nonlinearity of the NLN model was nearly linear in this case, and the total duration of the first-order kernel was only about two-thirds as long as in the dark-adapted situation.

In these terms, the behavior of a light-adapted photoreceptor is much simpler than a dark-adapted one, and the NLN model (with only second-order nonlinearity) fitted the responses quite well with a small residual mean square error. The output nonlinearity seems to be a simple compression, consistent with self-shunting of the membrane (Laughlin, 1981) enhanced by voltage-dependent mechanisms (Pece and French, 1992). Increased activation or deactivation of voltage-dependent  $K^+$  channels causes increased compression

of the membrane potential range in light-adapted blowfly photoreceptors (Weckström et al., 1991).

### The dark-adapted photoreceptor

Dark-adapted phototransduction had more significant nonlinearities, as expected. The second-order parallel cascade model was unable to account for a significant fraction of the output signal, and we must conclude that higher-order kernels contribute significantly to the response. Surprisingly, the strong second-order nonlinearity was almost entirely limited to the diagonal. Previous kernels obtained from white noise stimulation (Eckert and Bishop, 1975; Gemperlein and McCann, 1975; Marmarelis and McCann, 1977; Pece et al., 1990) and paired flash experiments (Pece et al., 1990) had significant off-diagonal components. These differences presumably arose from the different method used here, which tested the cells over a large part of their normal operating range.

In dark-adapted photoreceptors, both the input and output nonlinearities of the NLN sandwich model were significant, and we can suggest what kind of processes they represent. The strong nonlinear compression at the input may reflect the way in which the transduction units are organized in the photoreceptors. Photopigment is embedded in the membranes of thousands of microvilli, which have been suggested to act as phototransduction units (Howard et al., 1987). When many photons arrive simultaneously, the probability increases that a photon will be absorbed by a pigment molecule in a transduction unit that has just initiated a transduction cascade and cannot initiate another within a short time. Pigment self-screening works in a similar manner, although on a much shorter time scale.

Similar processes would also be expected to occur in light-adapted receptors, but the background light intensity of  $10^6$  ep/s means that the steps of light caused more limited changes in the numbers of photons being transduced, which might explain the more linear responses. It is difficult to explore this problem in isolation because nonlinear behavior occurs in photoreceptors transducing only two photons together, probably by membrane conductance changes (Dubs, 1981; Pece and French, 1992).

The nonlinearity at the output of the dark-adapted photoreceptor (Fig. 11) is interesting because of its odd direction and order. While the dominant nonlinear feature of both dark- and light-adapted receptors was compression or saturation (Figs. 1 and 7), the dark-adapted output nonlinearity increased more than linearly with its input amplitude. This suggests some form of cooperativity during the final stages of the transduction process. Since the voltage responses are produced by current flowing through light-gated ion channels, one possible source of cooperativity would be the activation of channels by some internal transmitter. The second-order characteristic of the nonlinearity could then be caused by a channel requiring two or more molecules to bind before opening. The light-gated channels have recently been shown by Hardie (1991) and Hardie and Minke (1992) to be

both calcium permeable and dependent on internal calcium. This may form part of the cooperative mechanism. In photoreceptor axons, signals are boosted by an independent mechanism (Weckström et al., 1992), and this effect might also be seen in the soma responses at high stimulus intensities.

## CONCLUSIONS

Phototransduction in fly photoreceptors is probably much more complex than the models of Fig. 4 would suggest. However, these simple nonlinear cascades can account for a considerable part of the response produced by a wide range of input light intensities, especially for light-adapted photoreceptors. Future work will be directed at testing associations between cascade components and physiological mechanisms, using techniques to modify photoreceptor functioning, such as pharmacological manipulation or mutant photoreceptors. These models should provide a useful basis for developing more complete descriptions of how the underlying physiochemical processes produce the final changes in membrane potential.

Support for this work was provided by the Medical Research Council of Canada and the Natural Sciences and Engineering Research Council of Canada.

## REFERENCES

- Autrum, H., editor. 1981. Light and dark adaptation in invertebrates. *In Handbook of Sensory Physiology VII/6C*. Springer-Verlag, Berlin. 1–91.
- Baylor, D. A., A. L. Hodgkin, and T. D. Lamb. 1974. The electrical responses of turtle cones to flashes and steps of light. *J. Physiol. (Lond.)* 242: 685–727.
- Classen-Linke, I., and H. Stieve. 1986. The sensitivity of the ventral photoreceptor of *Limulus* recovers after light adaptation in two phases of dark adaptation. *Z. Naturforsch.* 41c:657–667.
- Dubs, A. 1981. Non-linearity and light adaptation in the fly photoreceptor. *J. Comp. Physiol.* 144:53–59.
- Eckert, H., and L. G. Bishop. 1975. Nonlinear dynamic transfer characteristics of cells in the peripheral visual pathway of flies. Part I: The retinula cells. *Biol. Cybern.* 17:1–6.
- Fein, A., and E. Z. Szuts. 1982. Photoreceptors: Their Role in Vision. Cambridge University Press, Cambridge, England.
- French, A. S. 1979. The effect of light adaptation on the dynamic properties of phototransduction in the fly, *Phormia regina*. *Biol. Cybern.* 32:115–123.
- French, A. S. 1980. The linear dynamic properties of phototransduction in the fly compound eye. *J. Physiol. (Lond.)* 308:385–401.
- French, A. S., and M. Järvillehto. 1978. The dynamic behaviour of photoreceptor cells in the fly in response to random (white noise) stimulation at a range of temperatures. *J. Physiol. (Lond.)* 274:311–322.
- French, A. S., and J. E. Kuster. 1985. Nonlinearities in locust photoreceptors during transduction of small numbers of photons. *J. Comp. Physiol.* A156: 645–652.
- Fuortes, M. G. F., and A. L. Hodgkin. 1964. Changes in time scale and sensitivity in the ommatidia of *Limulus*. *J. Physiol. (Lond.)* 172:239–263.
- Gemperlein, R., and G. D. McCann. 1975. A study of the response properties of retinula cells of flies using nonlinear identification theory. *Biol. Cybern.* 19:147–158.
- Grzywacz, N. M., and P. Hillman. 1985. Statistical test of linearity of photoreceptor transduction processes: *Limulus* passes, others fail. *Proc. Natl. Acad. Sci. USA* 82:232–235.
- Hardie, R. C. 1979. Electrophysiological analysis of fly retina. I: Comparative properties of R1–6 and R7 and 8. *J. Comp. Physiol.* 129:19–33.
- Hardie, R. C. 1985. Functional organization of the fly retina. *In Progress in Sensory Physiology*. Vol 5. D. Ottoson, editor-in-chief. Springer-Verlag, Berlin. 1–79.
- Hardie, R. C. 1991. Whole-cell recordings of the light induced current in dissociated *Drosophila* photoreceptors: evidence for feedback by calcium permeating the light sensitive channels. *Proc. R. Soc. Lond. Ser. B Biol. Sci.* B245:203–210.
- Hardie, R. C., and B. Minke. 1992. The *trp* gene is essential for a light-activated  $Ca^{2+}$  channel in *Drosophila* photoreceptors. *Neuron* 8:643–651.
- Hardie, R. C., D. Voss, O. Pongs, and S. B. Laughlin. 1991. Novel potassium channels encoded by the shaker locus in *Drosophila* photoreceptors. *Neuron* 6:477–486.
- Howard, J., B. Blakeslee, and S. B. Laughlin. 1987. The intracellular pupil mechanism and photoreceptor signal to noise ratios in the blowfly, *Lucilia cuprina*. *Proc. R. Soc. Lond. Ser. B Biol. Sci.* B231:415–435.
- Hunter, I. W., and M. J. Korenberg. 1986. The identification of nonlinear biological systems: Wiener and Hammerstein cascade models. *Biol. Cybern.* 55:135–144.
- Järvillehto, M. 1979. Receptor potentials in invertebrate visual cells. *In Handbook of Sensory Physiology*, VII/6A. H. Autrum, editor. Springer-Verlag, Berlin. 315–356.
- Järvillehto, M., and F. Zettler. 1970. Micro-localisation of lamina-located visual cell activities in the compound eye of the blowfly *Calliphora*. *Z. Vgl. Physiol.* 69:134–138.
- Järvillehto, M., M. Weckström, and E. Kouvalainen. 1989. Signal coding and sensory processing in the peripheral retina of the compound eye. *In Neurobiology of Sensory Systems*. R. N. Singh, and N. J. Strausfeld, editors. Plenum Publishing Corp., New York. 53–70.
- Juusola, M. 1993. Linear and nonlinear contrast coding in light adapted blowfly photoreceptors. *J. Comp. Physiol.* A 172:511–521.
- Korenberg, M. J. 1973. Identification of biological cascades of linear and static nonlinear systems. *Proc. Midwest Symp. Circuit Theory*. 18.2:1–9.
- Korenberg, M. J. 1982. Statistical identification of parallel cascades of linear and nonlinear systems. *I.F.A.C. Symp. Ident. Sys. Param. Est.* 1:580–585.
- Korenberg, M. J. 1988. Identifying nonlinear difference equation and functional expansion representations: the fast orthogonal algorithm. *Ann. Biomed. Eng.* 16:123–142.
- Korenberg, M. J. 1991. Parallel cascade identification and kernel estimation for nonlinear systems. *Ann. Biomed. Eng.* 19:429–455.
- Korenberg, M. J., A. S. French, and S. Voo. 1988. White-noise analysis of nonlinear behavior in an insect sensory neuron: kernel and cascade approaches. *Biol. Cybern.* 58:313–320.
- Laughlin, S. B. 1981. Neural principles in the visual system. *In Handbook of Sensory Physiology VII/6B*. H. Autrum, editor. Springer-Verlag, Berlin. 133–280.
- Laughlin, S. B. 1989. The role of sensory adaptation in the retina. *J. Exp. Biol.* 146:39–62.
- Laughlin, S. B., and M. Weckström. 1989. The activation of a slow voltage-dependent potassium conductance is crucial for light adaptation in blowfly photoreceptors. *J. Physiol. (Lond.)* 418:200P.
- Marmarelis, P. Z., and V. Z. Marmarelis. 1978. Analysis of Physiological Systems. The White-Noise Approach. Plenum Publishing Corp., New York. 487 pp.
- Marmarelis, V. Z., and G. D. McCann. 1977. A family of quasi-white random signals and its optimal use in biological system identification. *Biol. Cybern.* 27:57–62.
- Payne, R., and J. Howard. 1980. Response of an insect photoreceptor: a simple log-normal model. *Nature (Lond.)* 290:415–416.
- Pece, A. E. C., and A. S. French. 1992. Sublinear summation of responses in locust photoreceptors. *J. Comp. Physiol.* 170:729–738.
- Pece, A. E. C., A. S. French, M. J. Korenberg, and J. E. Kuster. 1990. Nonlinear mechanisms for gain adaptation in locust photoreceptors. *Biophys. J.* 57:733–743.
- Pinter, R. B. 1966. Sinusoidal and delta function responses of visual cells of the *Limulus* eye. *J. Gen. Physiol.* 49:565–593.
- Press, W. H., B. P. Flannery, S. A. Teukolsky, and W. T. Vetterling. 1990. Numerical Recipes in C. Cambridge University Press, Cambridge, England.

- Sakai, H. 1992. White-noise analysis in neurophysiology. *Physiol. Rev.* 72: 491–505.
- Tsukahara, Y. 1980. Effect of intracellular injection of EGTA and tetraethylammonium chloride on the receptor potential of locust photoreceptors. *Photochem. Photobiol.* 32:509–514.
- Weckström, M., E. Kouvalainen, and M. Järvilehto. 1988. Non-linearities in response properties of insect visual cells: an analysis in time and frequency domains. *Acta Physiol. Scand.* 132:103–113.
- Weckström, M., R. C. Hardie, and S. B. Laughlin. 1991. Voltage-activated potassium channels in blowfly photoreceptors and their role in light adaptation. *J. Physiol. (Lond.)*. 440:635–657.
- Weckström, M., M. Juusola, and S. B. Laughlin. 1992. Presynaptic enhancement of signal transients in photoreceptor terminals in the compound eye. *Proc. R. Soc. Lond. Ser. B. Biol. Sci.* B250:83–89.
- Zettler, F. 1969. Die abhängigkeit des übertragungsverhaltens von frequenz und adaptionszustand, gemessen am einzelnen lichtezeptor von *Calliphora erythrocephala*. *Z. Vgl. Physiol.* 64:432–449.